

A Multi-decoder Neural Tracking Method for Accurately Predicting Speech Intelligibility

Rien Sonck¹, Bernd Accou¹, Tom Francart¹, Jonas Vanthornhout¹

¹ ExpORL, Dept. of Neurosciences, KU Leuven, Leuven, Belgium

jonas.vanthornhout@kuleuven.be

Abstract

Objective: electroencephalogram (EEG)-based methods have shown promise to predict behaviorally measured speech intelligibility, but accuracy and robustness generally fall short of standard behavioral test-retest procedures, which often yield test-retest differences of less than 1 dB. We introduce the multi-decoder method to predict speech reception thresholds (SRTs) from EEG recordings of speech listening. This method is designed for populations unable to perform behavioral tests, allowing an objective assessment of speech intelligibility in various listening environments and informing clinical decision-making, hearing aid fitting or assessment of patients with disorders of consciousness (DoC).

Approach: The multi-decoder method aggregates information from hundreds of decoders, each trained using different combinations of speech features and EEG preprocessing configurations to compute neural tracking neural tracking (NT), quantifying each decoder's ability to reconstruct speech signals from EEG. To train and test the decoders, we used data from 39 participants (7 men, 32 women), aged 18 to 24 years, with a total EEG recording duration of 29 minutes per participant. Each participant first completed a behavioral task to estimate their SRT. Subsequently, EEG recordings were acquired while they listened to speech presented at six different signal to noise ratios (SNRs), as well as a narrated story presented in quiet. The NT values from all decoders were then combined into a single high-dimensional feature vector per subject. Then a support vector regression (SVR) model was trained to learn the relationship between these NT vectors and the behavioral SRTs, with the goal of predicting individual SRTs from the NT vectors.

Main result: Predictions using the multi-decoder method correlated significantly ($r=0.647$, $p < 0.001$) with behavioral SRTs (NRMSE = 0.19); all differences stayed below 1 dB. shapley additive explanations (SHAP) analysis indicated that while all features contributed, the theta and delta frequency bands, early lags, and subject-specific decoders had a slightly greater influence on model predictions. Furthermore, we demonstrated that leveraging pretrained subject-independent (SI) decoders allows reducing EEG data collection for new participants to just 15 minutes, comprising 3 minutes of story listening and 12 minutes across six SNR conditions with 40 matrix sentences each—without sacrificing prediction accuracy.

Significance: The multi-decoder method introduced in this study outperforms previous EEG-based approaches. Future research should validate the method in more diverse clinical populations, including those with hearing loss.

1. Introduction

Assessing speech intelligibility, the extent to which a listener can understand spoken words and sentences, is a fundamental aspect of evaluating human auditory function. A widely used metric for this purpose is the speech reception threshold (SRT), defined as the signal to noise ratio (SNR) at which a listener can correctly repeat 50% of the presented speech material. SRTs are useful for evaluating hearing-impaired listeners, with or without hearing aids, in challenging listening environments (Festen & Plomp, 1986; Plomp, 1986; Verschuur & van Benthem, 1992), as well as for assessing the effectiveness of specific hearing aid algorithms (van Dijkhuizen et al., 1989; Zaar et al., 2024).

Behavioral SRT tasks, have been developed for various languages to assess speech intelligibility in noise. One early example is the Swedish matrix test (Hagerman, 1982), which has since inspired adaptations in multiple languages, including Dutch and Flemish (Houben et al., 2014; Luts et al., 2014). However, these behavioral assessments require active participation, which can be challenging or unfeasible when testing children or certain clinical groups. As a result, neuroimaging-based methods have gained interest in measuring speech intelligibility.

Neuroimaging studies have employed backward (i.e. decoder) and forward (i.e. encoder) models of neural tracking (for a review Gillis et al., 2022). These models seek to establish a linear mapping between the features of the speech stimulus (e.g., the envelope, the acoustic onsets, and the phonemes) and the corresponding brain responses. Backward models reconstruct the speech feature from the multichannel electroencephalogram (EEG) signal, whereas forward models predict the EEG signal for each channel from the stimulus feature. For backward models, the Pearson correlation between the reconstructed feature and the actual feature is called the neural tracking (NT) value. For forward models, this is the Pearson correlation between the reconstructed EEG signal and the actual EEG signal.

Perception of the speech envelope is important for speech intelligibility (Peelle & Davis, 2012; Shannon et al., 1995; Smith et al., 2002), which is further supported by studies showing a strong correlation between behaviorally measured speech intelligibility and neural tracking of the speech envelope (Vanthornhout et al., 2018). However, while broadband envelope perception is necessary for intelligibility, it is not always sufficient; spectro-temporal fine structure also plays an important role, especially in noisy or challenging listening conditions (Ding et al., 2014; Lorenzi et al., 2006; Moore, 2008). Decoding of the speech envelope is further influenced by factors such as spectral degradation (Karunathilake et al., 2023; Kösem et al., 2023), speech rate (Verschueren et al., 2022), attention (Vanthornhout et al., 2019) and binaural unmasking (Dieudonné et al., 2025). Notably, neural tracking of the envelope also oc-

cers for foreign or unintelligible speech (Gillis et al., 2023; Ortiz Barajas et al., 2021; Reetzke et al., 2021; Song & Iverson, 2016; Zou et al., 2019); nevertheless, the envelope remains an important acoustic feature for speech understanding.

While the speech envelope is an important feature for speech intelligibility, acoustic onsets also play a role in supporting speech understanding. Acoustic onsets are derived from the half-wave rectified first derivative of the speech envelope. Acoustic onsets are important for segmenting and organizing speech and carry essential phonetic information (Brodbeck et al., 2018; Kluender et al., 2003). Enhancing acoustic onsets in cochlear implants has been shown to improve speech intelligibility (Koning & Wouters, 2012, 2016). However, like the envelope, acoustic onsets are processed by the auditory system regardless of speech intelligibility (Karunathilake et al., 2023).

Currently, only a limited number of studies have proposed objective EEG-based methods for estimating speech intelligibility. Iotzov and Parra (2019) implemented a hybrid approach that combined forward and backward modeling to assess speech intelligibility; however, they did not attempt to estimate SRTs. They found that speech detection improved with intelligibility, as reflected by increased EEG–speech correlation. Approaches specifically designed to predict the SRT from EEG data began with the work of Vanthornhout et al. (2018), who employed a backward modeling approach. In this approach, neural tracking values were computed across a range of SNR conditions, and a sigmoid function was fitted to these values, analogous to fitting a psychometric curve in behavioral experiments. The midpoint of the fitted curve, referred to as the correlation threshold, was used as an estimate of the behavioral SRT, yielding a correlation of 0.69 between them, with a median absolute difference of 1.7 dB, and a standard deviation of 3.17 dB. However, the approach was not successful for all participants: in 21% of the cases (5 out of 24 subjects), the correlation threshold could not be reliably determined. An alternative approach using forward modeling was investigated by Lesenfants et al. (2019), who evaluated a variety of speech characteristics, including envelope, spectrogram, phonemes, phonetic characteristics and a combined feature set termed FS (phonetic characteristics + phonemes of the spectrogram). The FS feature provided the best performance and did not require sigmoid fitting. Instead, they introduced the FS-zero crossing, defined as the SNR at which the neural tracking values transitioned from negative to positive. This measure was effective for predicting behavioral SRTs and achieved a mean absolute difference of 0.97 dB. Another study using forward modeling was conducted by Borges et al. (2025), who used the envelope feature and also applied sigmoid fitting. Their method achieved a median difference of 0.38 dB with a standard deviation of 1.45 dB, but failed to reliably fit 9% of participants (2 out of 22). Muncke et al. (2022) predicted behavioral SRTs by combining forward models with a root mean square approach, eliminating the need for sigmoid fitting and achieving a mean difference of 1.2 dB.

While most work on deep learning and speech intelligibility does not directly estimate SRTs, one notable exception is the study by Accou et al. (2021). In this work, a dilated convolutional neural network was trained using a match–mismatch paradigm, and sigmoid fitting was used to estimate SRTs from classification accuracy across SRTs. This method achieved a correlation of 0.59 with the behavioral SRTs, a median absolute difference of 3.64 dB, and a standard deviation of 1.68 dB.

Despite recent advances, two main challenges remain. First, many existing approaches still struggle to provide reliable SRT predictions at the individual level. In contrast, the

behavioral matrix test consistently delivers accurate SRT measurements, with studies reporting very low test–retest variability—median differences around 0.4 dB (Boon, 2014) and a standard deviation of 0.7 dB (Decruy et al., 2018). While EEG-based methods are advancing and gradually closing this accuracy gap, they have yet to reach the robustness of behavioral benchmarks. Second, comparing SRT prediction performance across studies is difficult due to variations in speech material and differences in the distribution of behavioral SRTs among participants.

In this work, we propose a new method to tackle the first challenge: the multi-decoder method. The key innovation lies in combining information across a large set of decoders, each trained on differing configurations of stimulus features (envelope and acoustic onsets), integration windows (ranging from 0 to 500 milliseconds (*ms*)), frequency bands (delta, theta, and broadband), and both subject-specific and subject-independent decoder configurations. This removes the constraint of having to select these parameters in advance for all subjects. Furthermore, our method replaces traditional sigmoid fitting by combining the error function with a support vector regression (SVR) approach, enabling robust and accurate SRT predictions across all participants. Additionally, we analyze how much EEG data is necessary to maintain optimal model performance. Specifically, we want to know if pretrained subject-independent decoders can reduce the amount of EEG data we require from new participants to keep the same model performance in predicting their SRT—a crucial step toward practical application in clinical settings.

For the second challenge: to compare SRT prediction performance across speech material and SRT distributions, we advocate for more standardized reporting across studies. To this end, we propose using the normalized root-mean square error (NRMSE) as a metric, as it accounts for variability in the data distribution and enables more meaningful comparisons of SRT prediction performance.

2. Materials and methods

2.1. Participants

A total of 39 participants (7 men, 32 women), aged between 18 and 24 years ($\bar{x} = 21$, $SD = 1.8$), were included from the dataset described by Accou et al., 2024. All participants had hearing thresholds within the normal to slight hearing loss range, as confirmed by pure-tone air conduction audiometry. Most thresholds were ≤ 20 dB hearing level (HL) across 125–8000 Hz, with a small number between 21 to 30 dB HL. Prior to participation, all subjects provided written informed consent of the protocol approved by the Medical Ethics Committee UZ KU Leuven/Research (KU Leuven, Belgium; reference S57102).

2.2. Experimental Procedure

Each participant completed a series of tasks as detailed by Accou et al., 2024. For the present study, we analyzed data from one behavioral task (hereafter, the matrix behavioral task) and two EEG tasks: the story task and the matrix EEG task. All auditory stimuli were presented binaurally at 62 dB A. EEG data were recorded from 64 scalp electrodes at a sampling rate of 8192 Hz. For additional details on the EEG acquisition, see Accou et al., 2024. See *Figure 1* for an overview of the experimental procedure.

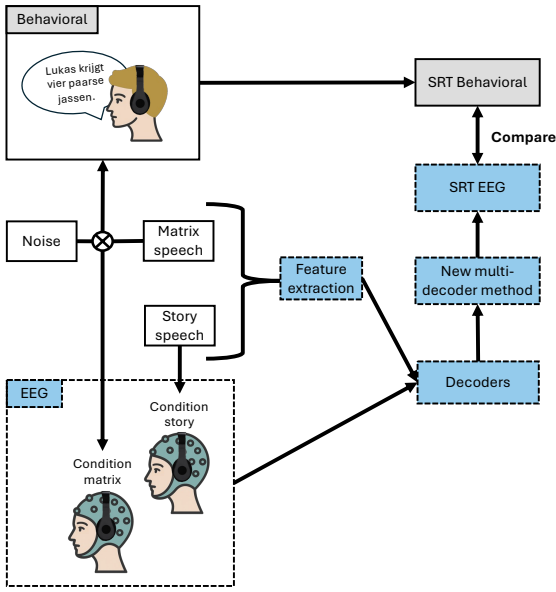


Figure 1: Overview of the experimental procedure. Each participant completed three main tasks: a behavioral task in which they listened to matrix sentences masked by speech-weighted noise and repeated them to determine their behavioral SRT; followed by two EEG tasks involving passive listening—one to a narrated story, and the other to matrix sentences presented with varying levels of speech-weighted noise. Feature extraction focused on the envelope and acoustic onsets of the clean stimuli. Both the stimulus features and the EEG recordings from the narrated story and matrix sentences were then used to train and test hundreds of different decoder configurations. These decoders were subsequently combined using our proposed multi-decoder method, which integrates information from all decoders to predict the SRT, allowing comparison with the behavioral SRT.

2.2.1. Matrix Behavioral Task

The Flemish matrix behavioral task (Luts et al., 2014) used an adaptive procedure to determine each participant’s SRT. Each test list consisted of 20 standardized sentences (one matrix list), presented against stationary speech-weighted noise fixed at 65 dB SPL. For full task details, see Luts et al. (2014).

2.2.2. Story Task

In the story task, participants listened to a 15-minute Flemish-language story, "Milan", narrated and written by Stijn Vranken, a male speaker, while their EEG was recorded.

2.2.3. Matrix EEG Task

During the matrix EEG task, participants listened attentively to matrix sentences presented in speech-weighted noise at fixed SNRs: $-12.5, -9.5, -6.5, -3.5, -0.5$, and 2.5 dB, as well as a silent condition. These are collectively referred to as the SNR conditions. Participants were told to listen passively. Each SNR condition comprised two matrix lists, totaling 40 sentences with brief pauses between them. All participants completed every SNR condition, and the order of conditions was randomized per participant. Each condition lasted approximately two minutes, resulting in a total task time of around 14 minutes.

2.3. Speech feature extraction

The speech signals were sampled at 48 kHz . The speech envelope and acoustic onset were extracted from clean versions of both the story and the matrix stimuli.

2.3.1. Envelope

To extract the temporal envelope (Env), the audio was processed with a gammatone filter bank using 28 subbands, with center frequencies from 50 Hz until 5000 Hz , followed by power-law compression: each subband envelope was calculated by taking the absolute value of each sample and raising it to the power of 0.6. The final broadband envelope was obtained by averaging across all subbands, using the same filter bank configuration as described by Biesmans et al. (2017) and Vanthornhout et al. (2018).

2.3.2. Acoustic onsets

Acoustic onsets (AEs) were computed as the first derivative of the speech envelope (that is, the difference between consecutive envelope samples) and applying half-wave rectification, which retains only positive changes.

2.4. Signal preprocessing

The EEG data were first high-pass filtered using a first-order zero-phase Butterworth filter with a cutoff frequency of 0.5 Hz . The data were then downsampled to 1024 Hz . Eye blink artifacts were removed using a multichannel Wiener filter (Somers et al., 2018), and any bad channels identified during the session EEG were linearly interpolated. The signals were re-referenced to the common average.

Both EEG, the envelope of the stimuli, and AE of the stimuli were downsampled to 64 Hz . Three least squares band pass filters (order 2000), each designed with a stopband attenuation of 80 dB and a passband ripple of 1 dB, were applied separately to extract the delta ($0.5\text{--}4\text{ Hz}$), theta ($4\text{--}8\text{ Hz}$), and broadband ($0.5\text{--}30\text{ Hz}$) frequency bands. Finally, all EEG channels

and speech features were z-score normalized across the whole recording.

2.5. Decoders

To assess how well the brain tracks or aligns with speech features, specifically the envelope and acoustic onsets of both the narrated story and matrix sentences, we used a decoder (i.e., backward model). This approach reconstructs speech features from neural data and compares them with the original speech features, providing a measure of neural tracking quantified by the Pearson correlation between the actual and reconstructed features (for a comprehensive overview, see Gillis et al., 2022). Once trained, the decoder can be applied to unseen neural data to reconstruct the corresponding stimulus feature. The resulting correlation coefficient serves as the neural tracking value: Higher correlations indicate a more accurate reconstruction of the stimulus feature from neural data, which can be interpreted as a marker of speech intelligibility for the participant (Vanthournhout et al., 2018).

2.5.1. Decoder configurations

A decoder configuration is defined by a set of parameters used to set up the decoder training and testing, including the EEG task (story vs. matrix), the speech feature (envelope vs. acoustic onsets), the integration window (27 windows), frequency bands (theta, delta, and broadband) and the type of decoder (subject-independent vs. subject-specific). Resulting in a total of 648 unique decoder configurations. Each decoder configuration is used to train and test seven decoders, one for each SNR condition: -12.5 , -9.5 , -6.5 , -3.5 , -0.5 , 2.5 dB, and silence, resulting in a total of 4536 decoders. For each decoder we used ridge regression to estimate the optimal set of weights (Machens et al., 2004) that maps the EEG data to the speech feature of interest, the speech envelope or the acoustic onsets. Although decoders can be trained on data from either the matrix or story EEG tasks, all decoders are exclusively tested on the matrix EEG task, as performance on this task provides the necessary information to predict the SRT.

The EEG task is defined in Section 2.2, the speech features in Section 2.3, and the frequency bands in Section 2.4. Below, we provide details on the post-integration window and the type of decoders.

2.5.2. Post-stimulus integration window

Because neural responses to sound occur with varying delays due to auditory processing latencies, the EEG data was expanded with multiple time-lagged versions of itself. This post-stimulus integration window was systematically varied from 0 to 500 ms. Sets of integration windows were constructed by starting at 0 and incrementally increasing the maximum time lag: first from 0 to 5 samples, then from 0 to 6 samples, and so on. At a sampling rate of 64 Hz, these correspond to lag ranges of 0–78 ms, 0–94 ms, 0–109 ms, etc., with each additional window extending the maximum lag by approximately 15 to 16 ms until 500 ms. Resulting in a total of 27 windows.

2.5.3. Decoder training

We used subject-independent (SI) and subject-specific (SS) decoders. The SI decoder was trained and evaluated across all participants using a leave-one-subject-out cross-validation (CV) approach (see *Figure 2A*). In this procedure, the data each participant served once as test data, while data from the remaining

participants were used for training. The decoder was trained using EEG data from either the story task or from a single SNR condition of the matrix task. As noted previously, each decoder was tested only on one corresponding SNR condition of the matrix task EEG data.

The SS decoder was trained and tested using data from a single participant (see *Figure 2B*). Two training configurations were used. In the first, the decoder was trained on the participant's EEG data from the story task and tested on one SNR condition of that participant's matrix task. In the second configuration, the decoder was both trained and tested on data from the same matrix task. As each SNR condition contained 40 matrix sentences, a leave-one-out sentence-wise cross-validation was applied: 39 sentences were used to train the decoder, and the remaining sentence was used for testing and feature reconstruction. This procedure was repeated until each sentence had been reconstructed once. The reconstructed stimulus features from all 40 test sentences were then concatenated—excluding silent intervals—and correlated with the corresponding actual stimulus features, yielding a single NT value.

2.6. Predicting the SRT

2.6.1. Adjusted neural tracking values

Each decoder configuration is used to train and test seven decoders, one for each SNR condition, resulting in seven neural tracking (NT) values: -12.5 , -9.5 , -6.5 , -3.5 , -0.5 , 2.5 dB, and silence, shown in (*Figure 3A*). The silence condition was excluded from further analysis, as neural responses to speech in noise differ fundamentally from those to speech in silence (Di Liberto & Lalor, 2017). The -12.5 dB SNR condition was chosen as a noise baseline, because it falls well below the SRT for all participants. NT values at this baseline were subtracted from the NT values at the other SNRs, resulting in five adjusted NT values for SNRs of -9.5 , -6.5 , -3.5 , -0.5 , and 2.5 dB, see *Figure 3B*.

2.6.2. Feature: ERF-adjusted NT vectors

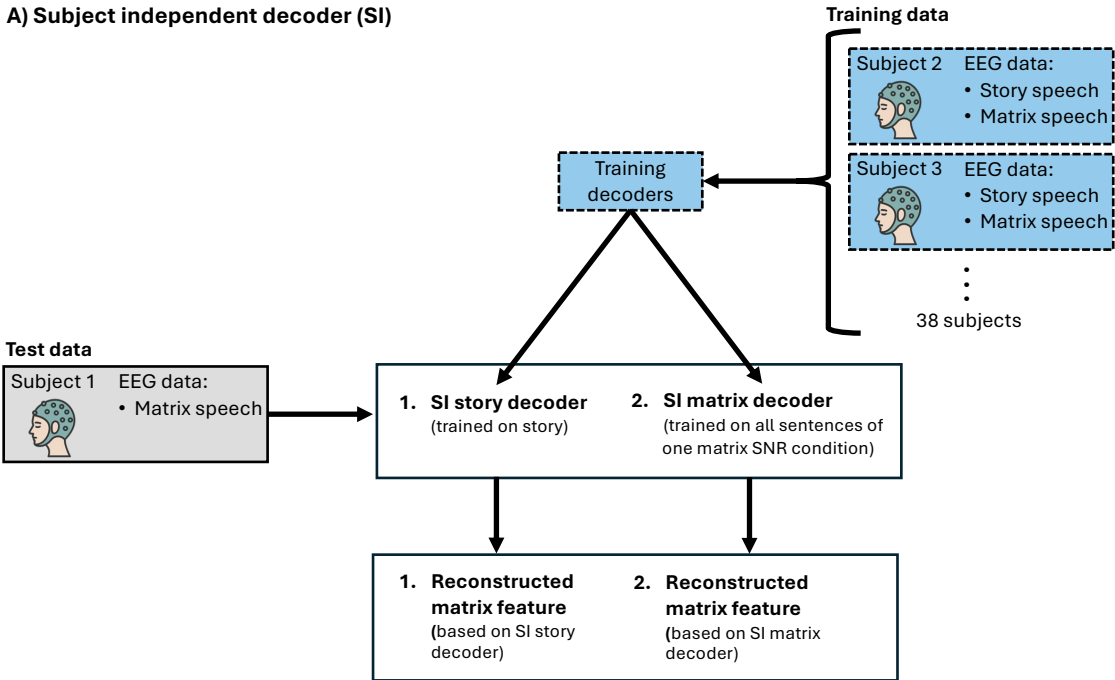
As each decoder configuration resulted in five adjusted NT values across SNRs, there are a total of 3240 adjusted NT values. For each subject, all these adjusted NT values are concatenated into a single, NT vector (see *Figure 3C*). The NT vector is then transformed using the error function (ERF) (Abramowitz & Stegun, 1972) (see *Figure 3D*), resulting in ERF-adjusted NT vectors. The ERF replaces the sigmoid fitting, transforming the curve into a smooth S-shape, similar to a psychometric function, but without requiring subject-specific curve fitting.

2.6.3. Model: support vector regression

Each participant was associated with an ERF-adjusted NT vector. To predict the corresponding SRT values from these vectors, a linear SVR model (Smola & Schölkopf, 2004) was used with ridge regularization and an efficient optimization algorithm based on L-BFGS (Ho & Lin, 2012; Hoerl & Kennard, 1970). This approach models the linear relationship between the ERF-adjusted NT vectors and the SRT outcomes, while controlling for overfitting through regularization.

Model performance was evaluated using a nested leave-one-out CV procedure to ensure unbiased hyperparameter tuning and testing. In the outer loop, one subject was held out as a test case, while the remaining subjects constituted the training set. Within this training set, an inner leave-one-out CV was performed, where one subject was used as a validation set to

A) Subject independent decoder (SI)



B) Subject specific decoder (SS)

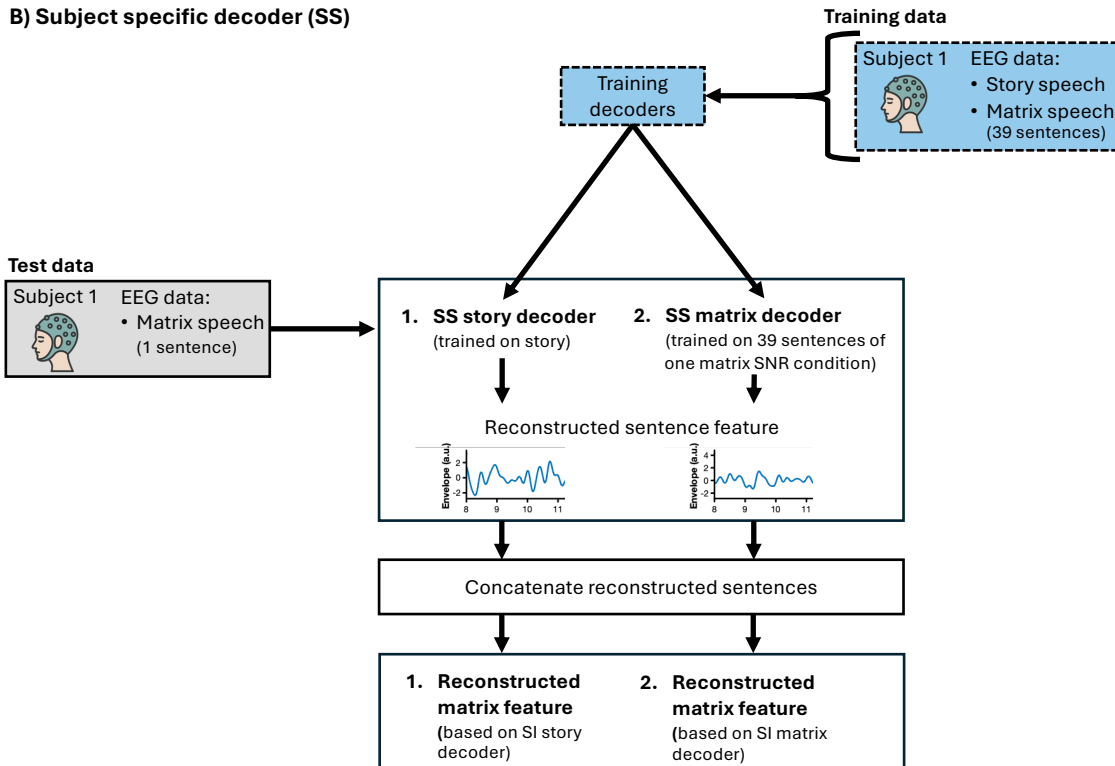


Figure 2: **Subject-independent and subject-specific decoders.** (A) For the SI decoder, leave-one-subject-out cross-validation is applied; this panel depicts the process for a single subject, representing one fold of the cross-validation. Two SI decoders are shown: one trained on EEG data from the story-listening task (SI story decoder) and another trained on EEG data from a specific SNR condition of the matrix listening task (SI matrix decoder). Each SNR condition includes two matrix sentence lists, totaling 40 sentences. (B) For the SS decoder, leave-one-out cross-validation was performed on matrix sentences within a single SNR condition. Similar to the SI decoders, two SS decoders were trained: one on EEG story data (SS story decoder) and one on EEG data from 39 of the 40 matrix sentences (SS matrix decoder). After reconstructing the features for all 40 sentences across the cross-validation folds, the reconstructed sentence features were concatenated into a single feature vector.

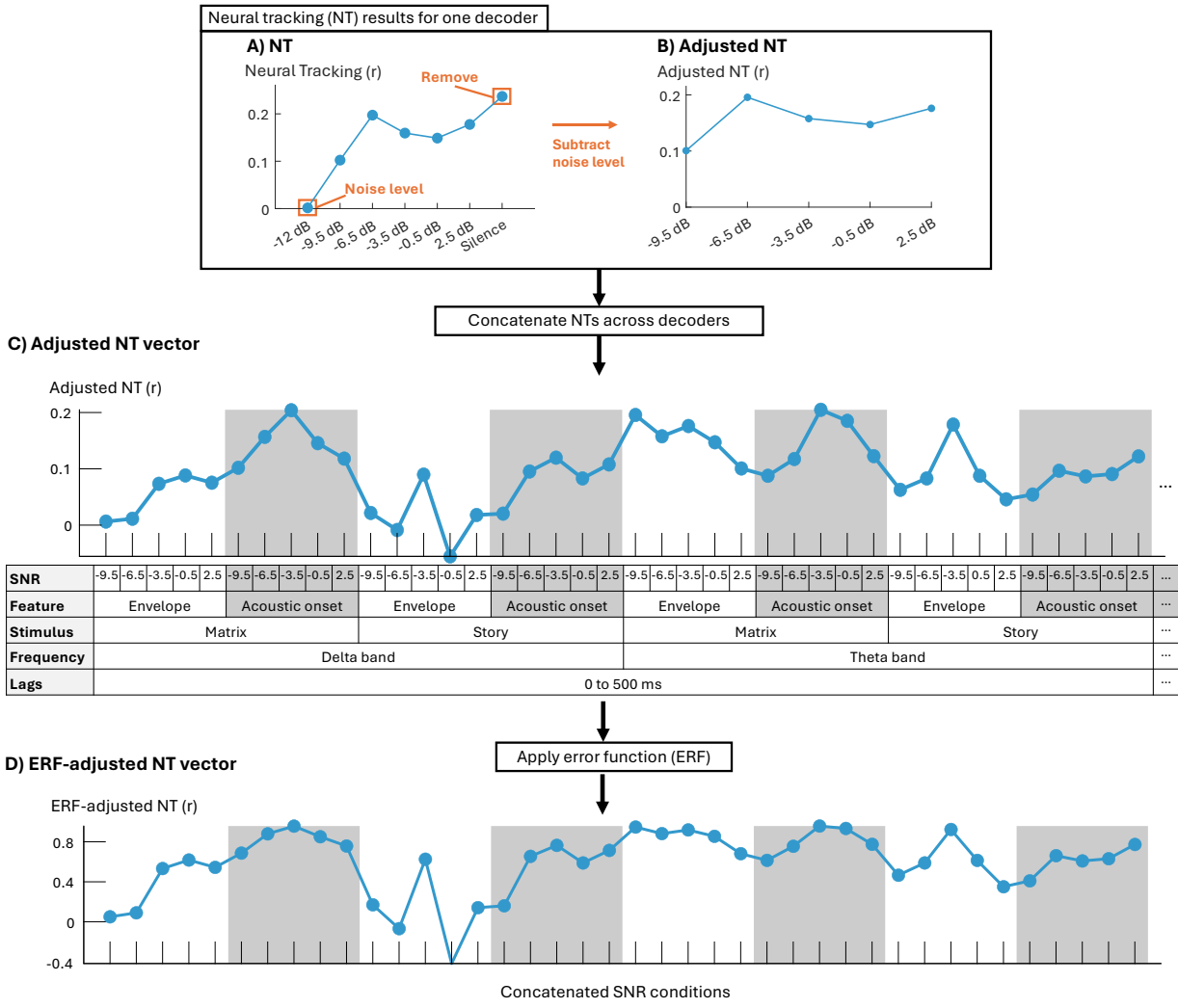


Figure 3: ERF-adjusted neural tracking vectors. (A) Displays NT values for seven SNR conditions using a specific decoder configuration (e.g., theta-band, story listening, stimulus envelope, lags up to 250 ms). Seven decoders—one per SNR condition—were trained and tested using the same decoder configuration, resulting in seven neural tracking values corresponding to each condition. The NT value at -12.5 dB SNR serves as the noise baseline, and the silence condition is excluded from further analysis. (B) Adjusted NT values are computed by subtracting the noise baseline (-12.5 dB SNR) from the NT values at the remaining SNR conditions. (C) Each decoder configuration produces its own set of adjusted NT values across the SNRs. These NT values from all decoder configurations are concatenated into a single comprehensive adjusted NT vector. The alternating grey and white backgrounds highlight the adjusted NT values corresponding to the same decoder configuration across different SNRs. For clarity, the decoder type parameter is not shown in this illustration. (D) Each subject's adjusted NT vector is transformed into an error function (ERF)-adjusted vector using the error function (ERF).

optimize the hyperparameter σ , which controls the steepness of the S-shaped error function curve. This curve models the expected neural tracking performance $\Psi(l)$ as a smooth sigmoid function of the stimulus SNR level l , centered at μ , the threshold or central SNR value:

$$\Psi(l) = \frac{1}{2} \left[1 + \text{erf} \left(\frac{l - \mu}{\sigma\sqrt{2}} \right) \right], \quad (1)$$

This ERF transformation was applied elementwise to each decoder configuration (grey and white background squares on (*Figure 3C*) of the NT vectors, following Equation (1). Importantly, the steepness parameter σ was fitted globally across all decoder configurations of the vector. This means that while every decoder configuration was individually transformed by the ERF function, the same fitted value of σ was used consistently across all decoder configurations.

Within each fold of the inner leave-one-out cross-validation loop, a different candidate value (ranging from 1 to 10) was tested. For each candidate, the adjusted NT vector was transformed into the ERF-adjusted NT vector. Subsequently, a support vector regression (SVR) model was trained on the inner training set and evaluated on the validation subject. The optimal σ was determined by minimizing the mean absolute error (MAE) between the true SRT (y_i) and the predicted SRT (\hat{y}_i) across all subjects in the inner loop:

$$MAE = \frac{1}{N} \sum_{i=1}^N |y_i - \hat{y}_i| \quad (2)$$

where N is the number of subjects in the inner loop. The σ that produced the lowest MAE was then selected, and the ERF with this optimal σ was applied to the adjusted NT vectors of all subjects in the training set. The SVR was then retrained on the entire outer training set and finally tested on the held-out test subject, resulting in a predicted SRT for that subject.

2.6.4. Model performance

Model performance was evaluated by correlating the predicted SRT values with the corresponding behavioral SRT measurements. To determine whether the observed correlation was statistically significant, we constructed a null distribution of model performance (*Figure A1*). This null distribution was generated by randomly shuffling the behavioral SRTs across participants, thereby breaking the relationship between the behavioral SRTs and the ERF-adjusted NT vectors. Using these shuffled data, we trained the SVR model anew using leave-one-out cross-validation to obtain a set of predicted SRTs, which were then correlated with the behavioral SRTs. This procedure was repeated 1000 times to yield a null distribution of correlation values. Because correlation coefficients are bounded between -1 and +1 and therefore non-normally distributed, we applied a Fisher Z-transformation to the null distribution. The resulting Z-transformed values approximate a normal distribution, enabling us to fit a Gaussian curve to the null data and perform statistical testing. Specifically, we calculated a two-tailed p-value by comparing the Fisher Z-transformed observed correlation to the null distribution.

Another way to evaluate model performance is by calculating the absolute difference between the predicted SRT and the behavioral SRT, as demonstrated by Lesenfants et al., 2019. This difference should ideally be less than 1 dB, comparable to the test-retest variability observed in the behavioral matrix task itself.

2.6.5. Evaluating the effect of data reduction on model performance

In this analysis, we aim to determine the minimum amount of EEG data required to maintain model performance comparable to using the full 27 minutes per subject (excluding the unused silence condition). To do this, we systematically reduced data from both the story and matrix EEG tasks.

For the matrix EEG task, we progressively reduced the number of matrix sentences per SNR condition from 40 down to 5, decreasing in steps of 5 sentences while keeping the full 15 minutes of story EEG data intact. This reduction affects both training and testing datasets involving matrix sentences.

For the story EEG task, we decreased the duration from 15 minutes to 3 minutes in 3-minute increments, while maintaining the complete set of 40 matrix sentences. This reduction impacts only the training data for the decoders, as all testing is performed only on the matrix EEG task data.

2.6.6. Performance comparison with other papers

To be able to compare the model performance with the performance obtained in other papers, we propose using the NRMSE as a metric, as it standardizes the variability of the different behavioral SRT distributions across papers:

$$\text{NRMSE} = \frac{\sqrt{\frac{1}{N} \sum_{i=1}^N (y_i - \hat{y}_i)^2}}{y_{\max} - y_{\min}} \quad (3)$$

where N is the number of observations, y_i are the behavioral SRT values, \hat{y}_i are the predicted SRT, and y_{\max} and y_{\min} are the maximum and minimum behavioral SRT values, respectively.

To obtain the behavioral and predicted SRTs from other studies, we extracted data points from published graphs using WebPlotDigitizer (Automeris) (Rohatgi, 2015). We were able to retrieve these values from the following papers: Accou et al., 2021; Borges et al., 2025; Vanthornhout et al., 2018.

2.6.7. SHAP analysis

Shapley additive explanations (SHAP) analysis (Lundberg & Lee, 2017) was used to interpret the contribution of each ERF-adjusted NT value to the prediction of the SRT outcome. To further explore model interpretability, these NT values were grouped by parameter combinations, allowing us to assess the relative importance of each lag, decoder type, stimulus feature, EEG task, and frequency band.

3. Results

3.1. SRT prediction

3.1.1. Behavioral

The participants' average SRT on the behavioral matrix test was -9.07 dB, with a standard deviation of 0.56 dB.

3.2. Model results

The SVR model, trained to learn a linear mapping between the ERF-adjusted NT vectors and behavioral SRTs, achieved a Pearson correlation of 0.647 ($p < 0.001$) between predicted SRTs and behavioral SRTs (see *Figure 4A*). The median absolute difference between predicted and behavioral SRTs was

0.29 dB, with a maximum difference of 0.91 dB, as shown in *Figure 4B*.

3.3. SHAP results

From the SHAP analysis (*Figure 5A-B*) it appears that while all parameters contribute, theta/delta bands, early lags, story stimulus, and the SS decoder have the strongest influence on model predictions.

3.4. Data reduction results

The data reduction analysis reveals that decreasing the number of matrix sentences in the matrix EEG task leads to an immediate decline in model performance, as shown in *Figure 6A*. In contrast, reducing the duration of the story EEG task does not affect performance; the relatively flat line indicates that model accuracy remains stable when the story EEG data is reduced from 15 to 3 minutes, see *Figure 6B*. *Figure 6* also demonstrates that combining both the SI and SS decoders is necessary to achieve the best model performance, outperforming the use of either decoder individually.

3.5. Comparison model results with other papers

Table 1 summarizes metrics from various studies. Although the current study does not demonstrate the highest correlation, it achieves the lowest NRMSE of 0.19 when the dataset variability is taken into account.

4. Discussion

We present a new method, the multi-decoder method, for predicting the SRT from subjects' EEG recordings obtained while listening to both matrix sentences and a continuous story. Central to this method is the introduction of ERF-adjusted NT vectors, these vectors captures NT information across a diverse set of decoder configurations.

Specifically, the NT vectors were constructed by varying key decoder parameters, including the EEG task and thus speech stimulus (story vs. matrix), the speech feature (envelope vs. acoustic onsets), the post-integration window (up to 500 ms), frequency bands (theta, delta, and broadband) and the type of decoder (subject-independent vs. subject-specific). This resulted in high-dimensional NT vectors. After noise-level subtraction and transformation with the error function, the resulting ERF-adjusted NT vectors were used in a SVR model to predict individual behavioral SRTs.

Using this model, we successfully predicted the SRT for all 39 participants, achieving a significant Pearson correlation of 0.647 between the predicted EEG-based SRT and the behavioral SRT. The median absolute difference between the predicted and behavioral SRTs across participants was 0.29 dB with a standard deviation of 0.26 dB, with this difference remaining below 1 dB for every individual.

The primary innovation of our approach lies in the integration of information from a wide array of decoders and feature sets. In contrast, previous methods typically relied on a single decoder type and feature set (Borges et al., 2025; Lesenfants et al., 2019; Muncke et al., 2022; Vanthornhout et al., 2018). Our method eliminates the need for sigmoid fitting, using a SVR instead. This change overcomes the limitations of some of the earlier methods, which often struggled to fit all subjects. Vanthornhout et al. (2018) could not fit 21% of the subjects (5 out of 24). Borges et al. (2025) could not fit 9% of the subjects (2

out of 22), Accou et al. (2021) could not fit 20% (4 out of 20) of the subjects and Lesenfants et al. (2019) could on average not fit 17% of the participants. However, both Lesenfants et al. (2019) and Muncke et al. (2022) proposed alternative methods that bypass sigmoid fitting, enabling SRT prediction for all participants. Lesenfants et al. (2019) combined time-aligned phonetic features with the spectrogram (Di Liberto et al., 2015), while Muncke et al. (2022) applied a time-windowed root mean square approach.

When comparing EEG-based models for predicting behavioral SRTs, it is important to consider the accuracy of the behavioral SRTs itself. Good quality speech materials has a behavioral test-retest differences are typically around 0.4 dB (median) with a standard deviation of 0.7 dB (Boon, 2014; Decruy et al., 2018). A challenge in comparing model performance across studies arises from the variability in behavioral SRT data between datasets, as illustrated in *Table 1*. Studies with lower SRT variability, including our own, may have an inherent advantage in achieving lower median dB differences between behavioral and predicted SRT. For example, a model that always predicts the average SRT would yield a lower median dB difference on datasets with smaller standard deviations compared to those with higher variability. To enable fairer comparisons, we recommend adopting metrics that normalize for dataset variability, such as the NRMSE. While previous studies did not report the NRMSE metric directly, we applied it retrospectively to their published results for a standardized comparison. These recalculated values are 0.86 (Vanthornhout et al., 2018), 0.52 (Borges et al., 2025), and 1.26 (Accou et al., 2021). In contrast, our multi-decoder approach achieves a substantially lower NRMSE of 0.19.

The SHAP analysis of the SVR model demonstrated that all parameters contribute to overall model performance; however, certain groups—specifically the theta and delta frequency bands, early lags, the story stimulus, and the SS decoder—exert a somewhat greater influence on the model's predictions. The prominence of early lags is not unexpected, as both speech features used in this study, envelope and acoustic onsets, are primarily bottom-up processed and less susceptible to top-down effects such as priming (Karunathilake et al., 2023). Both delta and theta bands play a crucial role in speech understanding, reflecting the brain's hierarchical processing of linguistic units such as sentences, phrases, words, syllables, and phonemes (Ding et al., 2016). This aligns with the modulation spectrum of natural speech, which contains prominent energy in the delta (1–4 Hz) and theta (4–8 Hz) ranges (Varnet et al., 2017).

This is further supported by previous findings, where the delta band was most predictive in Vanthornhout et al., 2018, while the theta band yielded the best results in Lesenfants et al., 2019. An interesting pattern emerges when comparing decoder types: SI decoders consistently achieve higher NT values across SNRs. This suggests that their advantage may be due to having access to a larger amount of training data, and that it is possible that SS decoders would reach similar NT values if provided with equivalent amount of data. In contrast, SS decoders yield higher SHAP values in the model, highlighting their greater contribution to predicting individual behavioral outcomes. This is further supported by the results that a multi-decoder method using only SS decoders performs much better than a multi-decoder method using only SI decoders. This suggests that SS decoders are better at capturing unique, individual-specific neural features that are particularly informative for predicting each subject's SRT.

In the present study, we initially used 29 minutes of EEG

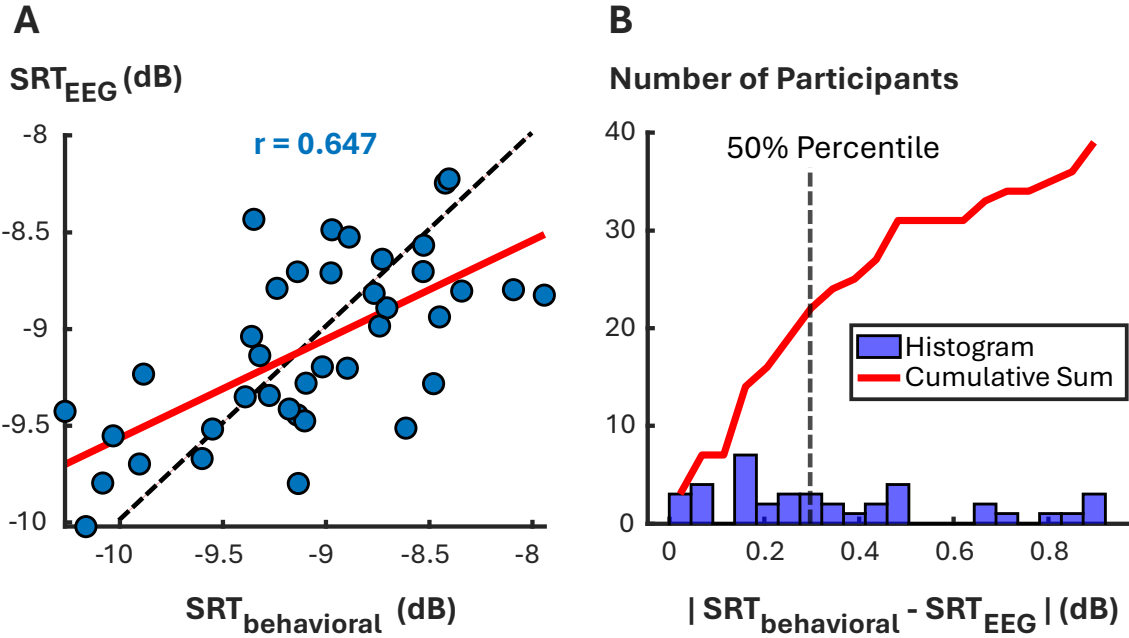


Figure 4: **Model performance results.** (A) Correlation ($p < 0.001$) between the behavioral SRT ($SRT_{behavioral}$) and the predicted SRT (SRT_{EEG}). The blue points are subjects, the red line is the regression fit, and the dotted line is the identity line. (B) Histogram of the absolute differences between $SRT_{behavioral}$ and SRT_{EEG} .

Table 1: Summary of behavioral and model performance metrics across studies, including mean and standard deviation (SD) of speech reception thresholds (SRT), correlation coefficients, median and standard deviation of the absolute dB differences, and normalized root mean square error (NRMSE). In this table, Sonck et al., 2026 refers to the current study.

N	Study	Mean SRT	SD SRT	Correlation	Median dB Diff.	SD dB Diff.	NRMSE
24	Vanthonhout et al., 2018	-7.6	1.48	0.69	1.7	3.17	0.86
19	Lesenfants et al., 2019		0.95				
18	Muncke et al., 2022		1.2				
20	Accou et al., 2023	-8.73	0.83	0.59	3.64	1.68	1.26
22	Borges et al., 2025	-5.34	0.6		0.38	1.45	0.52
39	Sonck et al., 2026	-9.07	0.56	0.65	0.29	0.91	0.19

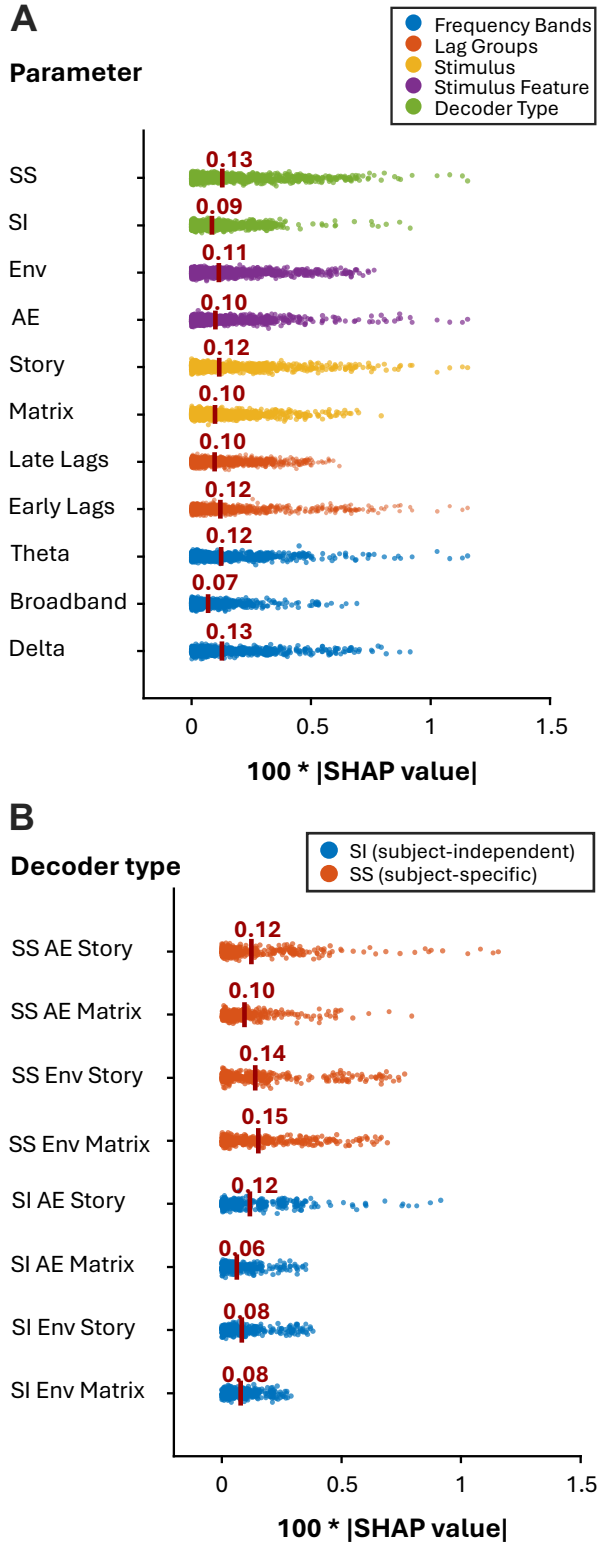


Figure 5: **SHAP analysis results.** Each point represents the SHAP value of a ERF-adjusted NT value for a specific parameter used in the decoder configuration. SHAP values are grouped as follows: (A) SHAP values are organized by parameter group. If a SHAP value corresponds to multiple parameters (e.g., both SS and Env), it appears in each relevant parameter group. (B) SHAP values are grouped according to the SS and SI decoders type.

data per subject. However, since the silence condition in the matrix EEG task was excluded, the effective recording time per participant was reduced to 27 minutes. Our time reduction analysis demonstrated that the duration of the story EEG task can be shortened from 15 to 3 minutes without compromising model performance, thereby reducing the total required EEG recording time to approximately 15 minutes. Conversely, reducing the number of matrix sentences in the matrix EEG task is not advisable, as this led to a decline in model accuracy. Consequently, when pretrained SI decoders are available from this dataset, it is feasible to predict a new participant’s SRT with only 15 minutes of EEG recording. Although this duration exceeds the time needed for a standard behavioral SRT test, it enhances feasibility for testing populations unable to perform behavioral assessments.

Thus, our proposed method shows potential for clinical application, particularly in populations where active participation is limited or not possible and support the evaluation of various hearing aid strategies. To further improve ecological validity, future research could omit matrix sentences and instead rely entirely on audiobook material presented at different SNR levels to predict SRTs, as suggested by Borges et al. (2025). Additionally, validating the multi-decoder method in individuals with hearing impairment and older adults would establish its generalizability across a wider range of SRTs, as the current findings are based solely on participants with normal hearing.

5. Conclusion

In this study, we introduced a the multi-decoder method, an EEG-based approach for predicting SRTs using ERF-adjusted NT vectors derived from a diverse set of decoders and with different decoder configurations. This approach enabled accurate SRT predictions for all participants resulting in a NRMSE of 0.19. SHAP analysis indicated that, while all parameters contributed to model performance, certain groups—specifically the theta and delta frequency bands, early lags, and SS decoders—had a somewhat greater influence. These results underscore the clinical potential of this method, particularly for populations where behavioral testing is difficult or impractical. Furthermore, we demonstrated that leveraging pretrained SI decoders allows reducing EEG data collection for new participants to just 15 minutes—comprising 3 minutes of story listening and 12 minutes across six SNR conditions with 40 matrix sentences each—without sacrificing prediction accuracy. Future research should evaluate and validate the method in more diverse clinical populations, including those with hearing loss.

6. References

- Abramowitz, M., & Stegun, I. A. (1972, December). Handbook of Mathematical Functions With Formulas, Graphs, and Mathematical Tables.
- Accou, B., Bollens, L., Gillis, M., Verheijen, W., Van hamme, H., & Francart, T. (2024). SparrKULee: A Speech-Evoked Auditory Response Repository from KU Leuven, Containing the EEG of 85 Participants. *Data*, 9(8), 94. <https://doi.org/10.3390/data9080094>
- Accou, B., Jalilpour Monesi, M., Van hamme, H., & Francart, T. (2021). Predicting speech intelligibility from EEG in a non-linear classification paradigm*. *Journal of Neural Engineering*, 18(6), 066008. <https://doi.org/10.1088/1741-2552/ac33e9>

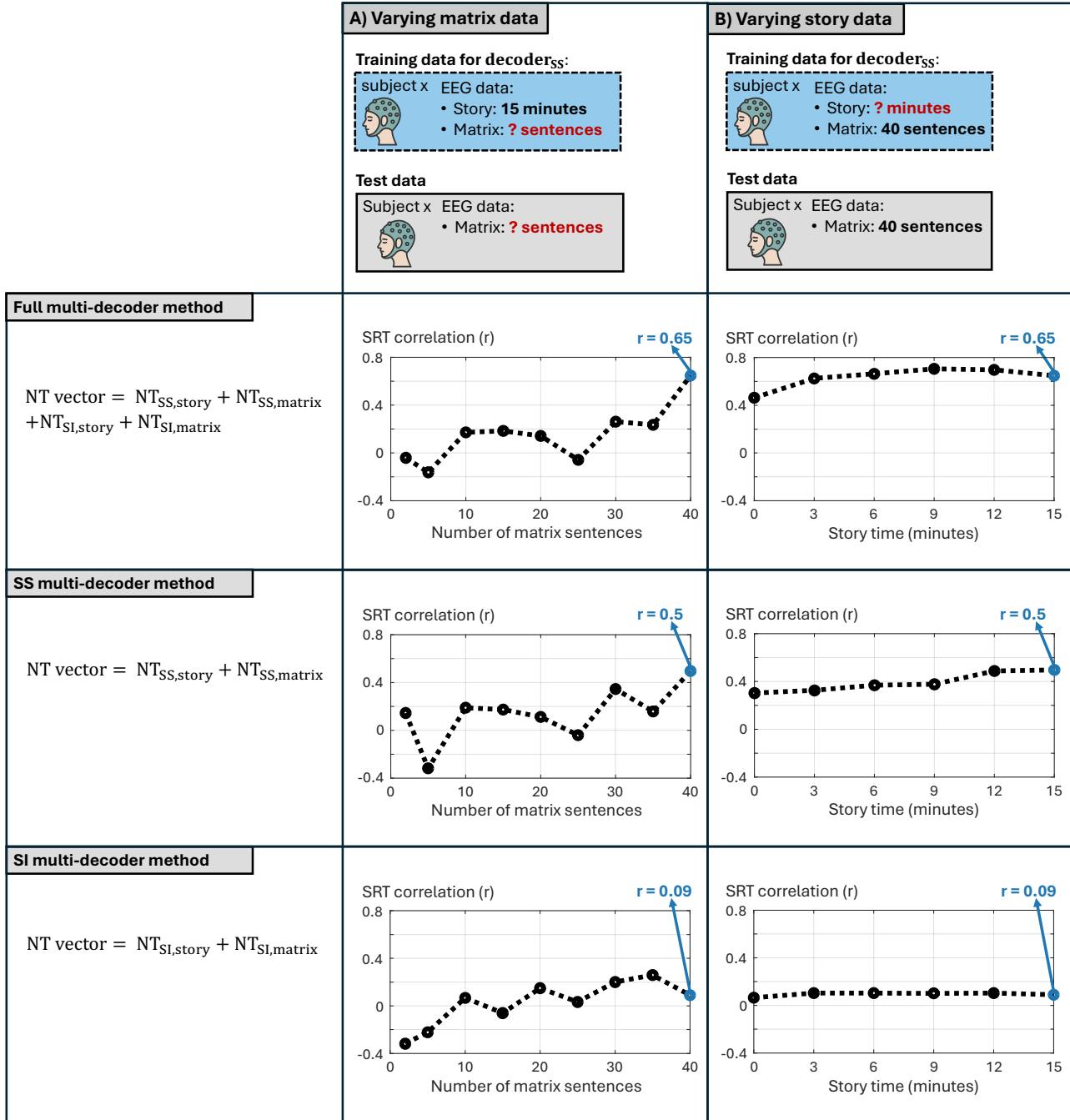


Figure 6: **EEG data reduction results.** (A) Illustrates the effect of reducing the amount of matrix EEG data, measured by the number of matrix sentences available to the model, while keeping the story EEG data constant at 15 minutes. The number of sentences cannot fall below 2, as the SS decoder requires at least one sentence for training and one sentence for testing. In the full multi-decoder method, the NT feature vector is constructed using outputs from both the SI and SS decoders. The SS multi-decoder method uses only SS decoders, whereas the SI multi-decoder method employs only SI decoders. (B) Shows the impact of reducing the amount of story EEG data on model performance, while keeping the number of matrix sentences constant at 40.

Accou, B., Vanthornhout, J., Hamme, H. V., & Francart, T. (2023). Decoding of the speech envelope from EEG using the VLAAI deep neural network. *Scientific Reports*, 13(1), 812. <https://doi.org/10.1038/s41598-022-27332-2>

Biesmans, W., Das, N., Francart, T., & Bertrand, A. (2017). Auditory-Inspired Speech Envelope Extraction Methods for Improved EEG-Based Auditory Attention Detection in a Cocktail Party Scenario. *IEEE Transactions on Neural Systems and Rehabilitation Engineering*, 25(5), 402–412. <https://doi.org/10.1109/TNSRE.2016.2571900>

Boon, S. (2014). *Multicenter evaluatie en validatie van de nieuwe Nederlandse Matrix* [Master's thesis, KU Leuven]. Unpublished; Not available online.

Borges, H. B., Zaar, J., Alickovic, E., Christensen, C. B., & Kidmose, P. (2025). Speech Reception Threshold Estimation via EEG-Based Continuous Speech Envelope Reconstruction. *The European Journal of Neuroscience*, 61(6), e70083. <https://doi.org/10.1111/ej.70083>

Brodbeck, C., Hong, L. E., & Simon, J. Z. (2018). Rapid transformation from auditory to linguistic representations of continuous speech. *Current biology : CB*, 28(24), 3976–3983.e5. <https://doi.org/10.1016/j.cub.2018.10.042>

Decruy, L., Das, N., Verschueren, E., & Francart, T. (2018). The Self-Assessed Békésy Procedure: Validation of a Method to Measure Intelligibility of Connected Discourse. *Trends in Hearing*, 22, 2331216518802702. <https://doi.org/10.1177/2331216518802702>

Di Liberto, G. M., & Lalor, E. C. (2017). Indexing cortical entrainment to natural speech at the phonemic level: Methodological considerations for applied research. *Hearing Research*, 348, 70–77. <https://doi.org/10.1016/j.heares.2017.02.015>

Di Liberto, G. M., O'Sullivan, J. A., & Lalor, E. C. (2015). Low-Frequency Cortical Entrainment to Speech Reflects Phoneme-Level Processing. *Current Biology*, 25(19), 2457–2465. <https://doi.org/10.1016/j.cub.2015.08.030>

Dieudonné, B., Decruy, L., & Vanthornhout, J. (2025). Neural tracking of the speech envelope predicts binaural unmasking. *The European Journal of Neuroscience*, 61(1), e16638. <https://doi.org/10.1111/ej.16638>

Ding, N., Chatterjee, M., & Simon, J. Z. (2014). Robust cortical entrainment to the speech envelope relies on the spectro-temporal fine structure. *NeuroImage*, 88, 41–46. <https://doi.org/10.1016/j.neuroimage.2013.10.054>

Ding, N., Melloni, L., Zhang, H., Tian, X., & Poeppel, D. (2016). Cortical tracking of hierarchical linguistic structures in connected speech. *Nature Neuroscience*, 19(1), 158–164. <https://doi.org/10.1038/nn.4186>

Festen, J. M., & Plomp, R. (1986). Speech-reception threshold in noise with one and two hearing aids. *The Journal of the Acoustical Society of America*, 79(2), 465–471. <https://doi.org/10.1121/1.393534>

Gillis, M., Van Canneyt, J., Francart, T., & Vanthornhout, J. (2022). Neural tracking as a diagnostic tool to assess the auditory pathway. *Hearing Research*, 426, 108607. <https://doi.org/10.1016/j.heares.2022.108607>

Gillis, M., Vanthornhout, J., & Francart, T. (2023). Heard or Understood? Neural Tracking of Language Features in a Comprehensible Story, an Incomprehensible Story and a Word List. *eNeuro*, 10(7). <https://doi.org/10.1523/ENEURO.0075-23.2023>

Hagerman, B. (1982). Sentences for testing speech intelligibility in noise. *Scandinavian Audiology*, 11(2), 79–87. <https://doi.org/10.3109/01050398209076203>

Ho, C.-H., & Lin, C.-J. (2012). Large-scale Linear Support Vector Regression. *Journal of Machine Learning Research*, 13(107), 3323–3348.

Hoerl, A. E., & Kennard, R. W. (1970). Ridge Regression: Biased Estimation for Nonorthogonal Problems. *Technometrics*, 12(1), 55–67. <https://doi.org/10.2307/1267351>

Houben, R., Koopman, J., Luts, H., Wagener, K. C., van Wieringen, A., Verschuur, H., & Dreschler, W. A. (2014). Development of a Dutch matrix sentence test to assess speech intelligibility in noise. *International Journal of Audiology*, 53(10), 760–763. <https://doi.org/10.3109/14992027.2014.920111>

Iotzov, I., & Parra, L. C. (2019). EEG can predict speech intelligibility. *Journal of Neural Engineering*, 16(3), 036008. <https://doi.org/10.1088/1741-2552/ab07fe>

Karunathilake, I. M. D., Kulasingham, J. P., & Simon, J. Z. (2023). Neural tracking measures of speech intelligibility: Manipulating intelligibility while keeping acoustics unchanged. *Proceedings of the National Academy of Sciences*, 120(49), e2309166120. <https://doi.org/10.1073/pnas.2309166120>

Kluender, K. R., Coady, J. A., & Kieft, M. (2003). Sensitivity to change in perception of speech. *Speech Communication*, 41(1), 59–69. [https://doi.org/10.1016/S0167-6393\(02\)00093-6](https://doi.org/10.1016/S0167-6393(02)00093-6)

Koning, R., & Wouters, J. (2012). The potential of onset enhancement for increased speech intelligibility in auditory prostheses. *The Journal of the Acoustical Society of America*, 132(4), 2569–2581. <https://doi.org/10.1121/1.4748965>

Koning, R., & Wouters, J. (2016). Speech onset enhancement improves intelligibility in adverse listening conditions for cochlear implant users. *Hearing Research*, 342, 13–22. <https://doi.org/10.1016/j.heares.2016.09.002>

Kösem, A., Dai, B., McQueen, J. M., & Hagoort, P. (2023). Neural tracking of speech envelope does not unequivocally reflect intelligibility. *NeuroImage*, 272, 120040. <https://doi.org/10.1016/j.neuroimage.2023.120040>

Lesenfants, D., Vanthornhout, J., Verschueren, E., Decruy, L., & Francart, T. (2019). Predicting individual speech intelligibility from the cortical tracking of acoustic- and phonetic-level speech representations. *Hearing Research*, 380, 1–9. <https://doi.org/10.1016/j.heares.2019.05.006>

Lorenzi, C., Gilbert, G., Carn, H., Garnier, S., & Moore, B. C. J. (2006). Speech perception problems of the hearing impaired reflect inability to use temporal fine structure. *Proceedings of the National Academy of Sciences of the United States of America*, 103(49), 18866–18869. <https://doi.org/10.1073/pnas.0607364103>

Lundberg, S. M., & Lee, S.-I. (2017). A Unified Approach to Interpreting Model Predictions. *Advances in Neural Information Processing Systems*, 30.

Luts, H., Jansen, S., Dreschler, W., & Wouters, J. (2014). Development and normative data for the Flemish/Dutch Matrix test. Available online: <https://lirias.kuleuven.be/retrieve/293640>.

Machens, C. K., Wehr, M. S., & Zador, A. M. (2004). Linearity of Cortical Receptive Fields Measured with Natural Sounds. *Journal of Neuroscience*, 24(5), 1089–1100. <https://doi.org/10.1523/JNEUROSCI.4445-03.2004>

Moore, B. C. J. (2008). The Role of Temporal Fine Structure Processing in Pitch Perception, Masking, and Speech Perception for Normal-Hearing and Hearing-Impaired People. *JARO: Journal of the Association for Research in Otolaryngology*, 9(4), 399–406. <https://doi.org/10.1007/s10162-008-0143-x>

Muncke, J., Kuruviila, I., & Hoppe, U. (2022). Prediction of Speech Intelligibility by Means of EEG Responses to Sentences in Noise. *Frontiers in Neuroscience*, 16. <https://doi.org/10.3389/fnins.2022.876421>

Ortiz Barajas, M. C., Guevara, R., & Gervain, J. (2021). The origins and development of speech envelope tracking during the first months of life. *Developmental Cognitive Neuroscience*, 48, 100915. <https://doi.org/10.1016/j.dcn.2021.100915>

Peelle, J. E., & Davis, M. H. (2012). Neural Oscillations Carry Speech Rhythm through to Comprehension. *Frontiers in Psychology*, 3. <https://doi.org/10.3389/fpsyg.2012.00320>

Plomp, R. (1986). A signal-to-noise ratio model for the speech-reception threshold of the hearing impaired. *Journal of Speech and Hearing Research*, 29(2), 146–154. <https://doi.org/10.1044/jshr.2902.146>

Reetzke, R., Gnanateja, G. N., & Chandrasekaran, B. (2021). Neural tracking of the speech envelope is differentially modulated by attention and language experience. *Brain and language*, 213, 104891. <https://doi.org/10.1016/j.bandl.2020.104891>

Rohatgi, A. (2015). Webplotdigitizer [Version 3.9, accessed Nov. 2025].

Shannon, R. V., Zeng, F.-G., Kamath, V., Wygonski, J., & Ekelid, M. (1995). Speech Recognition with Primarily Temporal Cues. *Science*, 270(5234), 303–304. <https://doi.org/10.1126/science.270.5234.303>

Smith, Z. M., Delgutte, B., & Oxenham, A. J. (2002). Chimaeric sounds reveal dichotomies in auditory perception. *Nature*, 416(6876), 87–90. <https://doi.org/10.1038/416087a>

Smola, A. J., & Schölkopf, B. (2004). A tutorial on support vector regression. *Statistics and Computing*, 14(3), 199–222. <https://doi.org/10.1023/B:STCO.0000035301.49549.88>

Somers, B., Francart, T., & Bertrand, A. (2018). A generic EEG artifact removal algorithm based on the multi-channel Wiener filter. *Journal of Neural Engineering*, 15, 036007. <https://doi.org/10.1088/1741-2552/aaac92>

Song, J., & Iverson, P. (2016). Cross-linguistic perception of continuous speech: Neural entrainment to the speech amplitude envelope. *The Journal of the Acoustical Society of America*, 140(4_Supplement), 3335. <https://doi.org/10.1121/1.4970635>

van Dijkhuizen, J. N., Festen, J. M., & Plomp, R. (1989). The effect of varying the amplitude-frequency response on the masked speech-reception threshold of sentences for hearing-impaired listeners. *The Journal of the Acoustical Society of America*, 86(2), 621–628. <https://doi.org/10.1121/1.398240>

Vanthornhout, J., Decruy, L., & Francart, T. (2019). Effect of Task and Attention on Neural Tracking of Speech. *Frontiers in Neuroscience*, 13.

Vanthornhout, J., Decruy, L., Wouters, J., Simon, J. Z., & Francart, T. (2018). Speech Intelligibility Predicted from Neural Entrainment of the Speech Envelope. *Journal of the Association for Research in Otolaryngology*, 19(2), 181–191. <https://doi.org/10.1007/s10162-018-0654-z>

Varnet, L., Ortiz-Barajas, M. C., Erra, R. G., Gervain, J., & Lorenzi, C. (2017). A cross-linguistic study of speech modulation spectra. *The Journal of the Acoustical Society of America*, 142(4), 1976. <https://doi.org/10.1121/1.5006179>

Verschueren, E., Gillis, M., Decruy, L., Vanthornhout, J., & Francart, T. (2022). Speech Understanding Oppositely Affects Acoustic and Linguistic Neural Tracking in a Speech Rate Manipulation Paradigm. *Journal of Neuroscience*, 42(39), 7442–7453. <https://doi.org/10.1523/JNEUROSCI.0259-22.2022>

Verschuur, J., & van Benthem, P. P. (1992). Effect of hearing aids on speech perception in noisy situations. *Audiology: Official Organ of the International Society of Audiology*, 31(4), 205–221. <https://doi.org/10.3109/00206099209081656>

Zaar, J., Simonsen, L. B., & Laugesen, S. (2024). A spectro-temporal modulation test for predicting speech reception in hearing-impaired listeners with hearing aids. *Hearing Research*, 443, 108949. <https://doi.org/10.1016/j.heares.2024.108949>

Zou, J., Feng, J., Xu, T., Jin, P., Luo, C., Zhang, J., Pan, X., Chen, F., Zheng, J., & Ding, N. (2019). Auditory and language contributions to neural encoding of speech features in noisy environments. *NeuroImage*, 192, 66–75. <https://doi.org/10.1016/j.neuroimage.2019.02.047>

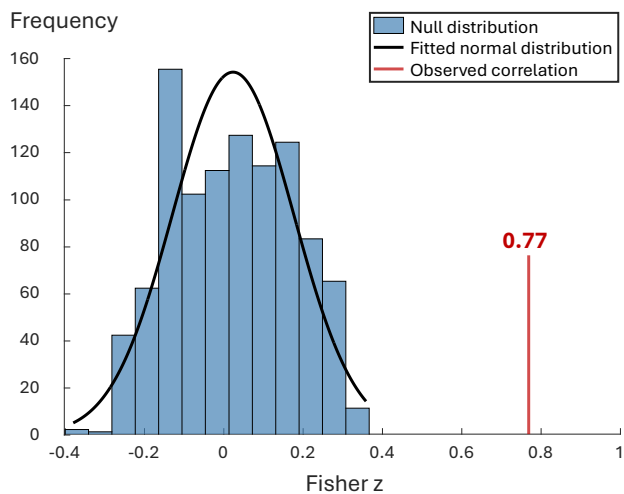


Figure A1: **Null distribution.** The distribution of Fisher Z-transformed null correlations has a mean of 0.02 and a standard deviation of 0.15. The observed correlation, also Fisher Z-transformed and calculated from the model without disrupting the underlying data structure (indicated by the red line), falls significantly outside this null distribution. This indicates a statistically meaningful relationship beyond chance.